SUPPLEMENTARY FIGURES AND TABLES

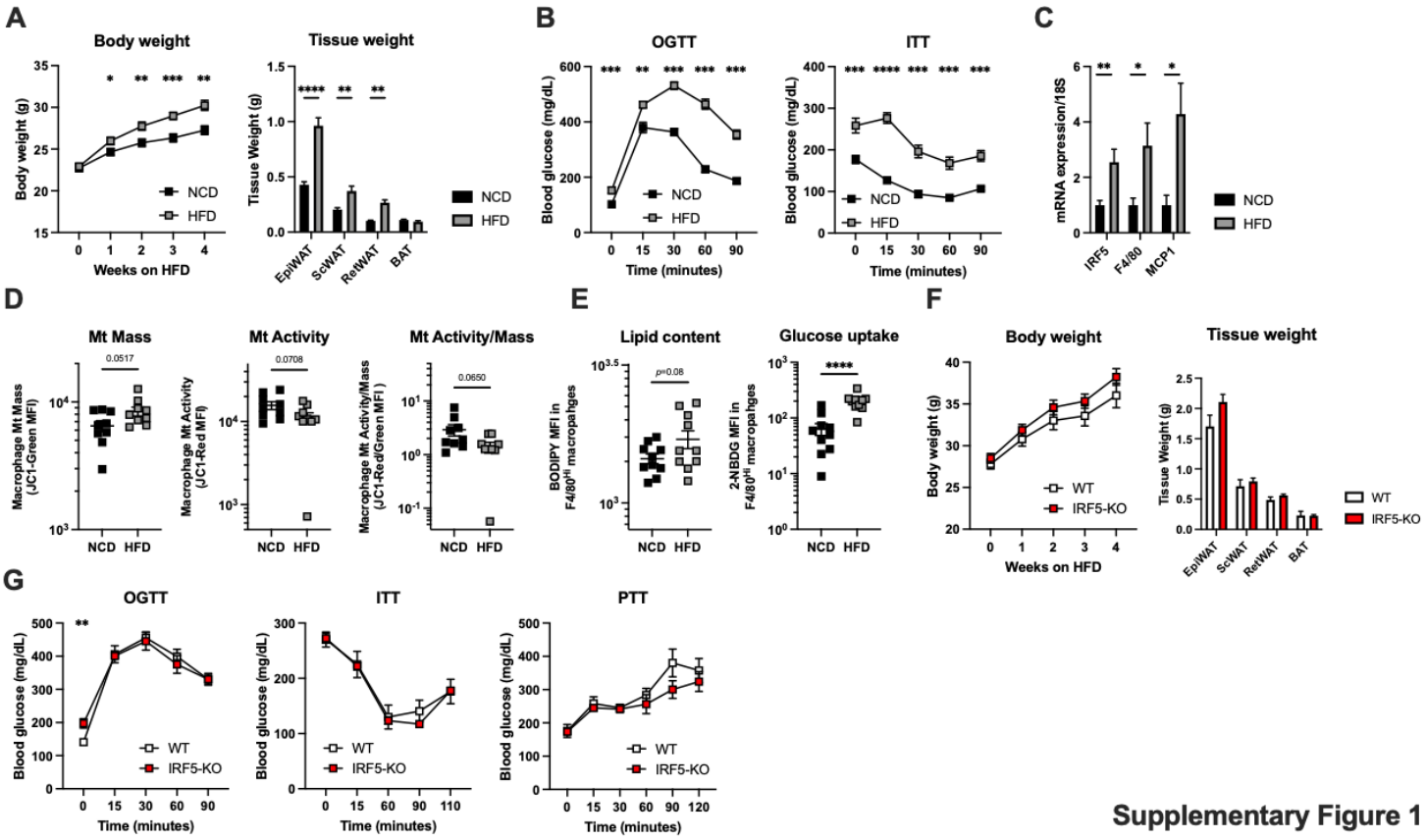

Supplementary Figure 1

Supplementary Figure S1. Short-term caloric excess affects systemic metabolism and alters adipose tissue macrophage metabolism. Supplementary to Figure 1. **A.** Weight of C57BL/6J mice on high-fat diet (HFD) or normal chow diet (NCD) for 4 weeks (n=10 per group, *p=0.0186, ***p=0.0008, ***p=0.0001, two-way ANOVA). Epididymal white adipose tissue (EpiWAT), subcutaneous white adipose tissue (ScWAT), retroperitoneal white adipose tissue (RetWAT) and brown adipose tissue (BAT) weight from C57BL/6J mice on HFD and NCD (n=10 per group, ****p<0.0001, **p=0.0065, **p=0.0078, two-way ANOVA). **B.** Oral glucose tolerance test (OGTT) and insulin tolerance test (ITT) on mice following HFD or NCD (n=10 per group, for OGTT ***p=0.0006, **p=0.0015, ****p<0.0001, two-way ANOVA. For ITT ***p=0.0008, ****p<0.00001, ***p=0.000013, ***p=0.000038, ***p=0.00016 two-way ANOVA). **C.** IRF5, F4/80 and MCP1 mRNA expression in EpiWAT of mice on HFD or NCD (n=10 per group, **p=0.006, *p=0.02, *p=0.01 unpaired t-test). **D.** FACS analysis of EpiWAT adipose tissue macrophage (ATM) mitochondrial (Mt) mass, Mt activity, Mt Activity-to-Mass ratio following HFD or NCD (n=9 per group, p-values as noted, unpaired t-test). **E.** FACS analysis of EpiWAT F4/80^{Hi} ATM lipid content and glucose uptake following HFD or NCD (n=10 per group, p value as stated, ****p<0.0001, unpaired t-test). **F.** Weight of mice with a myeloid-deficiency of IRF5 (IRF5-KO) or their wild-type (WT) littermates on HFD for 4 weeks. EpiWAT, ScWAT, RetWAT and BAT weight from IRF5-KO and WT mice following HFD (n=10 for WT and n=12 for IRF5-KO, unpaired t-test). **G.** OGTT, ITT and pyruvate tolerance test (PTT) on IRF5-KO and WT mice following HFD (WT n=8, IRF5-KO n=4 for GTT and ITT, n=4 per group for PTT, two-way ANOVA).

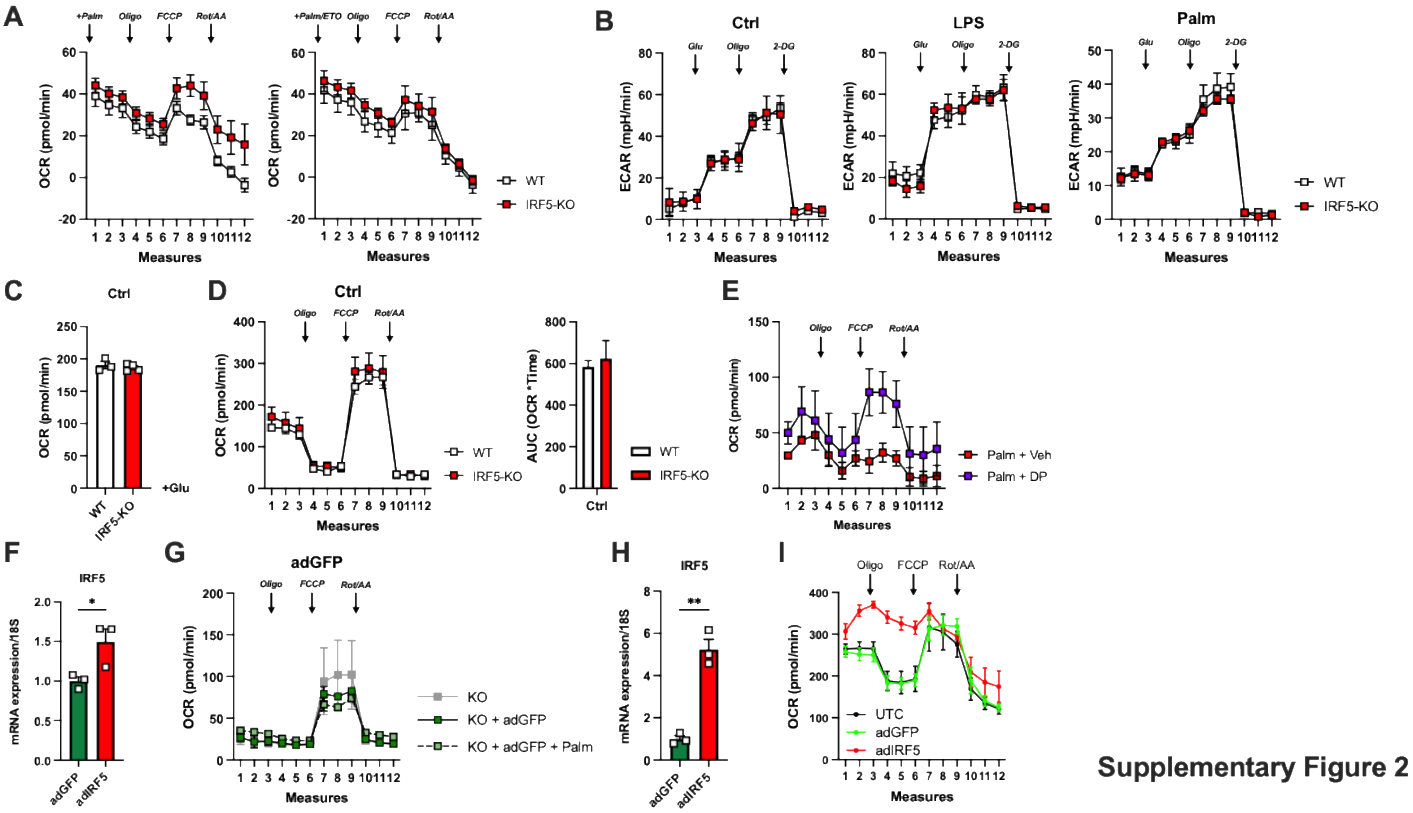

Supplementary Figure 2

Supplementary Figure S2. Myeloid-deficiency of IRF5 alters stromal vascular cell and bone marrow-derived macrophage respiration. Supplementary to Figure 2. **A.** Fatty acid oxidation test in EpiWAT SVF from WT (n=7) and IRF5-KO (n=9) following 4 weeks of HFD. Palm, palmitate; Oligo, oligomycin; FCCP, carbonyl cyanide 4-(trifluoromethoxy) phenylhydrazone; Rot/AA, rotenone/antimycin A; ETO, etomoxir. **B.** Glycolysis stress test measuring extracellular acidification rate (ECAR) of bone marrow-derived macrophages (BMDM) from WT and IRF5-KO mice upon administration of glucose (Glu), Oligo and 2-deoxyglucose (2-DG). BMDMs were untreated (Ctrl) or treated with lipopolysaccharides (LPS) or Palmitate (Palm), n=3 per condition for WT BMDMs and n=4 per condition for IRF5-KO. **C.** Oxygen consumption rate (OCR) from glycolysis stress following Glu injection in S2B. **D.** Mitochondrial stress test and OCR AUC of BMDMs from WT (n=3) and IRF5-KO (n=3) under basal (Ctrl) conditions. **E**. OCR measures from mitochondrial test of BMDMs following treatment with IRF5-decoy peptide (DP) or vehicle (Veh) and treatment with Palm (n=5 per condition) in Fig. 2J and 2K. **F.** BMDMs from IRF5-KO mice were treated with an IRF5 adenovirus (adIRF5) or a control adenovirus (adGFP). IRF5 RNA expression was quantified (n=3 per group; *=0.04, unpaired t-test). **G.** Metabolic flux analysis of BMDMs from IRF5-KO mice were treated with an adGFP and with Palm (n=3 per group). **H.** Primary brown adipocytes were treated with adIRF5 or adGFP. RNA expression of IRF5 was quantified (n=3 per condition; **p=0.001 unpaired t-test). **I.** OCR of mitochondrial stress test on primary brown adipocytes treated with adIRF5 (n=7), adGFP (n=7) or left without treatment (n=4 UTC, untreated control).

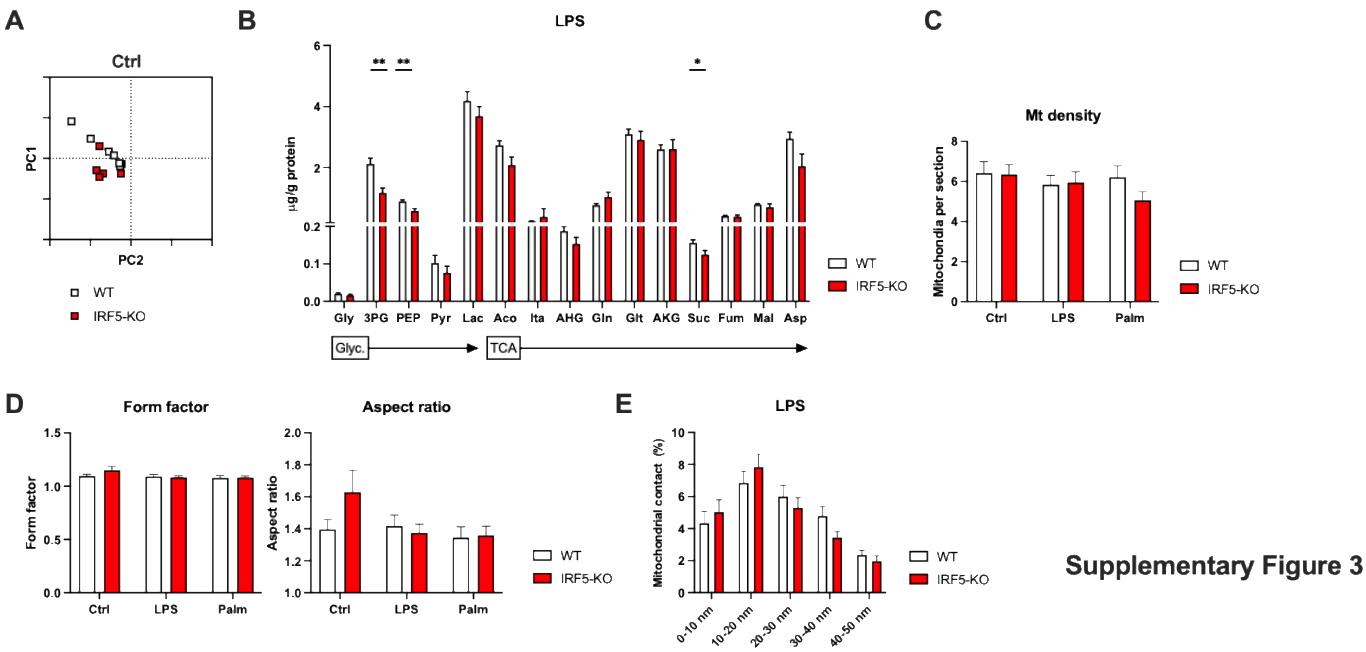

Supplementary Figure S3. IRF5-deficiency alters TCA metabolite response but not mitochondrial structural dynamics in response to LPS treatment. Supplementary to Figure 3. Bone marrow-derived macrophages (BMDM) from IRF5-KO or WT mice were treated with either LPS or palmitate (Palm) for 2 or 24 h. Targeted metabolomics analyses were carried out to quantify intracellular tricarboxylic acid (TCA) cycle intermediates and electron microscopy was carried out to evaluate mitochondrial structural characteristics (n=3 per condition). **A.** Principal component analysis (PCA) was carried out on TCA cycle intermediates (Fig. 3B). PCA plot represents samples under basal (Ctrl) conditions. **B.** Absolute quantification of TCA cycle metabolites in BMDMs from WT and IRF5-KO mice following treatment with LPS for 2 h. (left to right: **p=0.004, **p=0.006, *p=0.038). **C.** Analysis of mitochondrial density from electron micrographs in WT and IRF5-KO BMDMs (Fig. 3G) treated with LPS or Palm for 2h or in untreated controls (Ctrl). **D.** Analysis of mitochondrial form factor and aspect ratio from electron micrographs in WT and IRF5-KO BMDMs treated with LPS or Palm for 2 h or in untreated controls (Ctrl). **E.** Percentage of mitochondrial membrane in contact with endoplasmic reticulum (ER) at different mitochondria-ER contact (MERC) site distances in BMDMs from WT and IRF5-KO mice following 2-hour treatment with LPS.

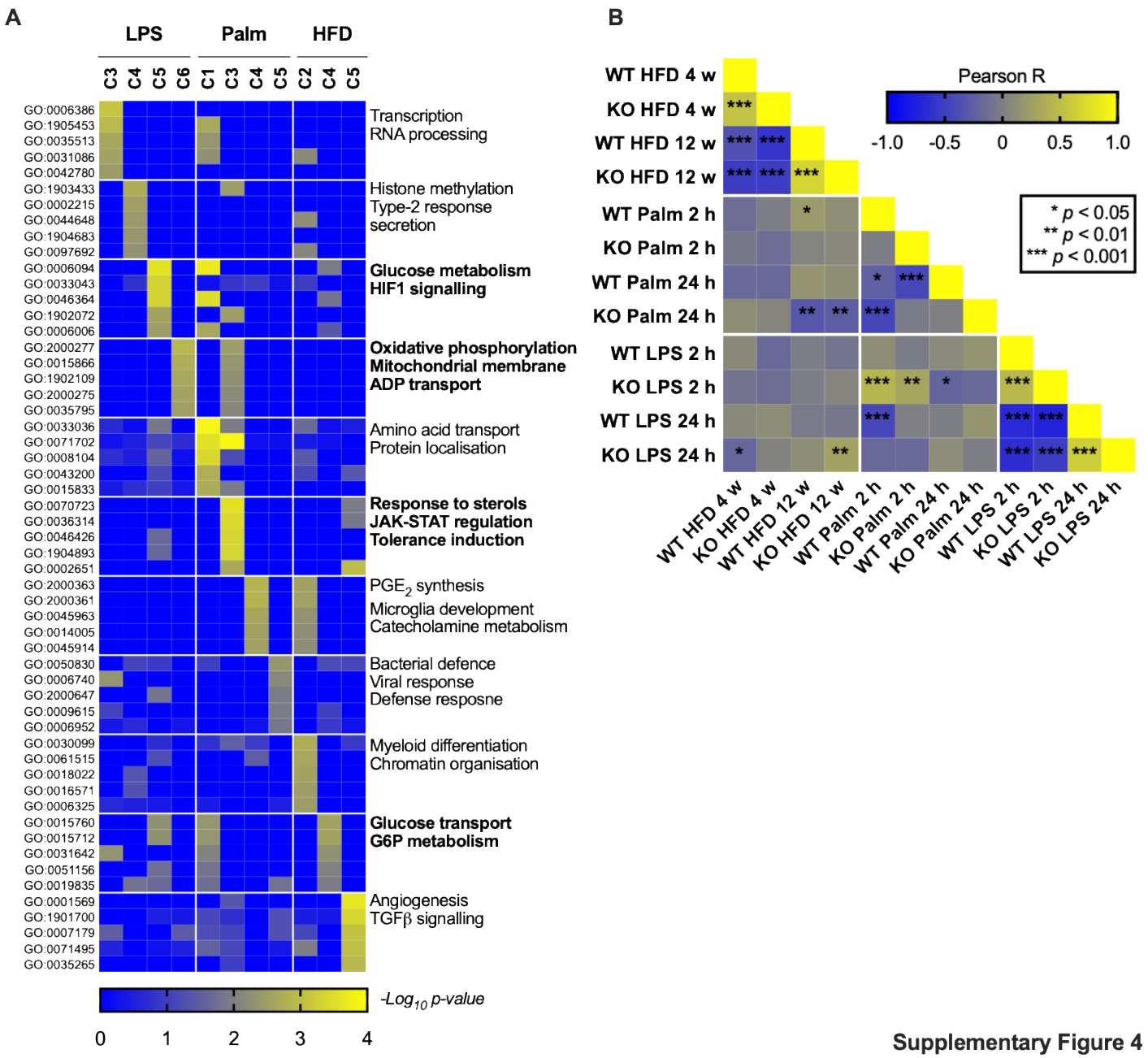

Supplementary Figure 4

Supplementary Figure S4. IRF5-deficiency alters the expression of genes related to cellular metabolism. Supplementary to Figure 4. **A.** Gene ontology (GO) term enrichment of genes from differentially regulated clusters in Fig 4B. Gene sets and clusters were generated from RNA sequencing of bone marrow-derived macrophages (BMDMs) from mice with a myeloid-deficiency of IRF5 (IRF5-KO) and their WT littermates treated for 2 or 24 h with LPS or palmitate (Palm) and epididymal white adipose tissue (EpiWAT) macrophages (ATMs) from IRF5-KO and WT mice following high-fat feeding for 4 or 12 weeks. **B.** Correlation matrix of normalised mRNA expression of coregulated differentially expressed genes between IRF5-KO and WT macrophages in Fig 4B.

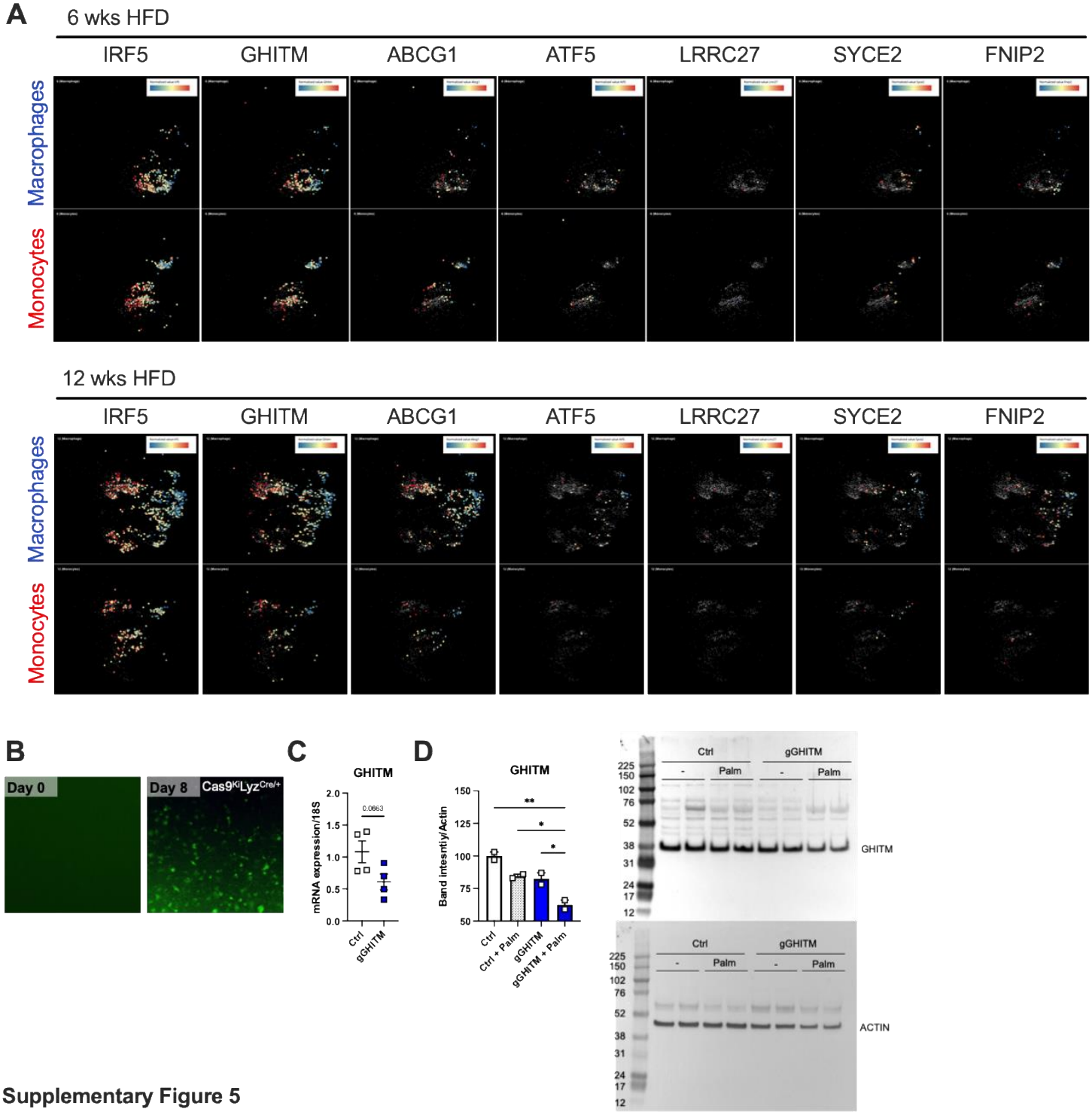

Supplementary Figure 5

Supplementary Figure S5. GHITM is highly expressed in epididymal visceral white adipose tissue macrophages and monocytes relative to other IRF5 targets. Supplementary to Figure 5. **A.** Public dataset of single-cell RNA sequencing of the epididymal white adipose tissue stromal vascular fraction of C57BL/6J mice following 6 or 12 weeks of high-fat feeding. Macrophages and monocytes were identified and expression of IRF5, of GHITM and of ABCG1, SYCE2, FNIP2, ATF5 and LRRC27 were projected onto tSNE plots per cell type and duration of high-fat feeding. **B.** Fluorescent image of bone marrow-derived macrophages (BMDM) from mice with myeloid-restricted Cas9-GFP at day 0 and day 8 of differentiation (20 x magnification). **C**. Gene expression of GHITM, IRF5, TNF and IL10 in

Cas9-expressing BMDMs treated with lipofection agent (Ctrl) or with a gRNA targeting GHITM (gGHITM) (n=4 per condition, unpaired t-test. *p=0.028). **D.** Quantification of western blotting against GHITM in the same experiment as Fig. 5E (n=2 per condition, one-way ANOVA. **p=0.0046, *p=0.031, *p=0.043).

SUPPLEMENTARY TABLES

Table S1. Genotyping primers

Genotyping		
IRF5 WT	F	CGT GTA GCA CTC CAT GCT CT
	R	AGG GCC TGT CCA GAA TTAGG
Irf5 Mut	F	CTT CGT ATA GCA TAC ATT ATACG
	R	AGG GCC TGT CCA GAA TTAGG
LyzM WT	F	TTA CAG TCG GCC AGG CTG AC
	R	CTT GGG CTG CCA GAA TTTCTC
LyzM Mut	F	CCC AGA AAT GCC AGA TTA CG
	R	CTT GGG CTG CCA GAA TTTCTC
Cas9 cre std WT	F	AAGGGAGCTGCAGTGGAGTA
	R	CAGGACAACGCCCACACA
Cas9 cre std MUT	F	CTTCTTCTTTGGGGCCATCT
	R	TCCCCATCAAGCTGATCC

Table S2. Surface markers for FACS analyses

Antibody	**Dye**	**Clone**	**Reference**
Human			
HLA-DR	Vioblue	AC122	Miltenyi ; 130-095-293
CD19	BV510	HIB19	BioLegend ; 302242
CD14	PE-Cy7	M5E2	BioLegend ; 301814
CD16	APC	3G8	BioLegend ; 302012
CD45	APC-eFluor780	HI30	eBioscience ; 47-0459-42
CD31	BV510	M89D3	BD ; 744463
CD11c	PerCP-Cy5.5	Bu15	Biolegend ; 337209
CD206	APC	15-2	BioLegend ; 321110
Mouse			
Antibody	Dye	Clone	Reference
CD206	BV421	C068C2	Biolegend ; 141717
CD19	BV510	6D5	Biolegend ; 115546
CD3	BV510	17A2	Biolegend ; 100234
CD45	PE-eF610	30-F11	Invitrogen ; 61-0451-82
F4/80	PE-Cy7	BM8	Invitrogen ; 25-4801-82
CD11c	APC	N418	Invitrogen ; 17-0114-81
CD11b	APC-Cy7	M1/70	Biolegend ; 101226

Table S3. Sequence-specific primers for quantitative RT-PCR

Murine primers		
Irf5	F	GATGGGGACAACACCATCTT
	R	GGCTTTTGTTAAGGGCACAG
TNF	F	CCACCACGCTCTTCTGTCTA
	R	CACTTGGTGGTTTGCTACGA
IL6	F	TACCACTTCACAAGTCGGAGGC
	R	CTGCAAGTGCATCATCGTTGTTC
GHITM	F	CTGCATTCTGGTGTGATGGG
	R	TGAGTACAGAGTGGCACCAG
F4/80	F	CCTTGGGAGCCTTCTGGATC
	R	CATCTGTGGCTGCCTCCCT
MCP1	F	GGGCCTGCTGTTCACAGTT
	R	CCAGCCTACTCATTGGGAT
18S	F	GGGAGCCTGAGAAACGGC
	R	GGGTCGGGAGTGGGTAATTT
Human primers		
GHITM	F	TTCCATCACGAAGAATCAATGGC
	R	CCATAGTAGCACAATGCTCCAA
IRF5	F	CTCTTGTTAAGGGCACAGC
	R	AACACCATCTTCAAGGCCT
18S	F	TTCGAACGTCTGCCCTATCAA
	R	ATGGTAGGCACGGCGACTA